


Proceedings Article

Flexible Software for Rigorous Simulations of Magnetic Particle Imaging Systems

Klaus Natorf Quelhas ^{a,b,c,*}. Mark-Alexander Henn^{a,d}. Tinh Q. Bui^a. Hunter R. Wages^e.
Weston L. Tew^a. Solomon I. Woods^a

^aNational Institute of Standards and Technology (NIST), Gaithersburg, MD 20899, USA

^bInstituto Nacional de Metrologia, Qualidade e Tecnologia (Inmetro), Rio de Janeiro, Brazil

^cUniversidade Federal do Rio de Janeiro (UFRJ), Rio de Janeiro, Brazil

^dUniversity of Maryland, College Park, MD 20742, USA

^eDrexel University, Philadelphia, PA 19104, USA

*Corresponding author, email: klaus.quelhas@nist.gov

© 2022 Quelhas *et al.*; licensee Infinite Science Publishing GmbH

This is an Open Access article distributed under the terms of the Creative Commons Attribution License (<http://creativecommons.org/licenses/by/4.0>), which permits unrestricted use, distribution, and reproduction in any medium, provided the original work is properly cited.

Abstract

Modeling of Magnetic Particle Imaging (MPI) systems allows for developing and testing novel methods for image reconstruction and simulating various setups without the need of real-life measurement data. Here we describe the the initial development of a C++ simulation software designed to provide more realistic MPI simulation data. Effects like non-linear gradient fields, non-uniform drive fields, space-dependent coil sensitivity, temperature gradients and particle relaxation are included in the simulations. In addition to MPI, the software is also suitable for simulating other applications, e.g., Magnetic Particle Spectroscopy (MPS), AC susceptibility and pulsed relaxometry. The comparison of the simulated signals against real-life MPS measurements is also shown in this work.

I. Introduction

Magnetic Particle Imaging (MPI) can provide quantitative mapping of magnetic nanoparticle (MNP) tracers in three-dimensional space for use in biomedical imaging and materials research [1]. The technique exploits the non-linear magnetization response of these MNPs when exposed to time-varying magnetic fields to provide high temporal and spatial resolution and highly sensitive three-dimensional maps, free from the influence of the surrounding material or tissue [2].

Modeling of MPI systems allows for developing and testing novel methods for image reconstructions without the need of real-life measurement data [3], and enables prototyping through the simulation of the response of different instrument setups. One limitation of typical model-based approaches is insufficiently accounting for

the non-ideal behavior of the elements that compose the experiments that are being modeled. This work describes an MPI simulation software developed to allow simulating non-linear gradient fields, non-uniform drive fields, space-dependent coil sensitivity, non-uniform sample temperature and particle relaxation by simulating permanent magnets, active and passive coils, as well as particle response. In addition, we describe the comparison of the software's results against real Magnetic Particle Spectroscopy (MPS) measurement data to ensure the generation of reliable data for testing new image reconstruction algorithms.

II. Material and methods

The simulation software was developed using the C++ language following an object-oriented programming

structure in such a way that each element of the simulated measurement system was modeled by a specific class.

The fields are generated either by permanent magnets or coils. For cylindrical magnets and solenoids, employed for generating *field-free points* (FFPs), the fields are computed in terms of a generalized elliptic integral [4]. For rectangular magnets, like the ones employed for producing *field-free lines* (FFLs), the method for computing the field was adapted from [5].

For the receive coils, the same expressions employed for the field generated by solenoids can be employed for computing the induced signal. The sensitivity $\mathbf{R}(\mathbf{x})$ is defined as the field the coil would produce at the position \mathbf{x} when driven by an unitary current. It can be employed for either computing the field generated by a current I or the voltage induced by a time-varying magnetization $\mathbf{M}(t)$ [6].

The information relative to the samples - particle characteristics, concentration, temperature and relaxation time - are stored in discrete *voxel* arrays with variable dimensions and sizes. This implies that each *voxel* responds independently to the applied field, which gives the necessary flexibility to simulate different grids with different particles and temperature gradients, as well as to study the effect of relaxation over the measured signal. The magnetization vector for the grid's i th *voxel* is given by the Langevin equation:

$$\mathbf{M}_i(t) = \rho_i m_i \left\{ \coth(k_i |\mathbf{H}_i(t)|) - \frac{1}{k_i |\mathbf{H}_i(t)|} \right\} \frac{\mathbf{H}_i(t)}{|\mathbf{H}_i(t)|} \quad (1)$$

where ρ_i is the particle concentration, m_i is the magnetic moment magnitude in Am^2 , $\mathbf{H}_i(t)$ is the applied field vector in A/m and $k_i = \mu_0 m_i / k_B T_i$, where μ_0 is the vacuum permeability, k_B is the Boltzmann constant and T_i is the voxel temperature in Kelvin.

Relaxation is implemented by means of a magnetization history array - each *voxel* has an array containing the previous adiabatic magnetization vectors, with the size of the array proportional to the particle relaxation time divided by the sampling time interval. The *voxel* is then "excited" by the applied magnetic field at each iteration, which allows the computation of the new relaxed magnetization vector by applying an exponential relaxation kernel to the adiabatic magnetization array.

The N individual *voxel* magnetizations are used to compute the magnetic flux ϕ_M across the receive coil due to the MNP sample:

$$\phi_M(t) = \mu_0 \sum_{i=1}^N \mathbf{R}(\mathbf{x}_i) \cdot \mathbf{M}_i(t), \quad (2)$$

where $\mathbf{R}(\mathbf{x}_i)$ is the coil sensitivity vector with relation to the *voxel* position x_i . Assuming i) that the gradient field is static and thus does not contribute to the induced EMF and ii) that the drive field is uniform over the receive coil

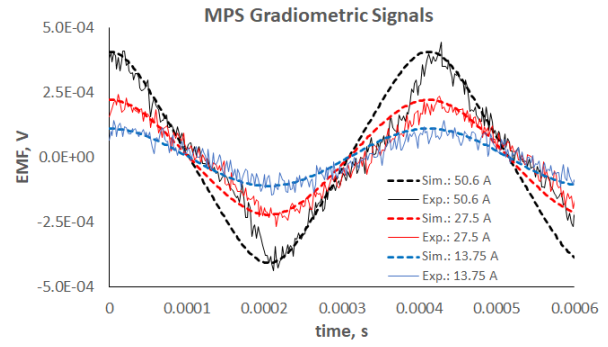


Figure 1: Comparison between the simulated (thick dashed lines) and measured (thin solid lines) MPS signals for different excitation currents and a frequency of 2427 Hz.

area, the flux due to the applied drive field \mathbf{H}_d is given by

$$\phi_{H_d}(t) = \mu_0 A_r [\mathbf{H}_d(t) \cdot \mathbf{a}_r] \quad (3)$$

where A_r is the area of the receive coil's cross section and \mathbf{a}_r is the coil's normal direction vector. The induced signal on the receive coil is then calculated from the computed changes in $\phi = \phi_M + \phi_{H_d}$ along the simulation:

$$s(t) = -d\phi(t)/dt \quad (4)$$

where

$$\frac{d\phi(t)}{dt} = \frac{(\phi(t) - \phi(t - \Delta t)) + (\phi(t + \Delta t) - \phi(t))}{2\Delta t} \quad (5)$$

It is possible to record the voltages induced by only the particles, only the drive field coils only or both. It is important to note that this computational strategy allows not only simulating 1D, 2D and 3D MPI measurements, but also MPS, alternating-current (AC) magnetic susceptibility and pulsed relaxometry measurements.

III. Results and discussion

During the development of the software, each C++ class was thoroughly tested and compared against finite element analysis (FEA) software or real measurement data. The fields computed for the FFP generation were compared to the ones generated by a FEA program for the same configuration: these differences were found as being less than 4 % for the whole space between the magnets.

The evaluation of the software as a whole when employing all active and passive elements together was performed by comparing the simulation results to the MPS experiment reported in [7]. The results of this evaluation are shown in Figure 1, demonstrating the good agreement between the simulated and measured signals. These results, together with a simulation of effects like space-dependent coil sensitivity and particle relaxation

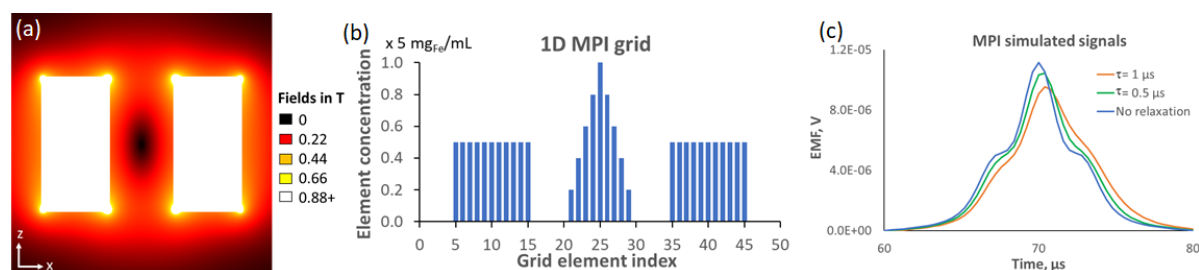


Figure 2: Simulation of a 1D MPI system. A cross section of a FFP generated by a pair of cylindrical permanent magnets is shown in (a). The 1D simulated grid is shown in (b), it is 10 mm long and composed of 51 *voxels* containing 20 nm magnetite particles at 273 K and a concentration up to 5 mg/mL of Fe. The simulated signals generated by this grid under a 5 T/m gradient field is shown in (c) for different relaxation times, being generated by a 25 mT drive signal in the x axis at 25 kHz.

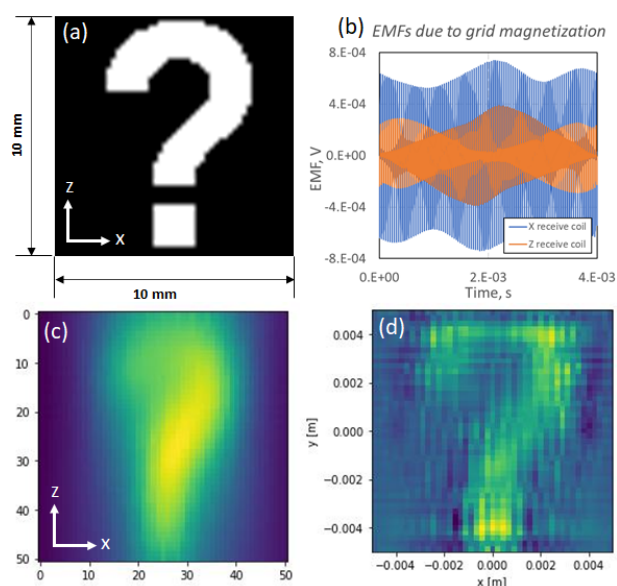


Figure 3: Simulation of a 2D MPI system. The concentration grid adopted for the simulation is shown in (a), while the time-domain simulated raw signal is shown in (b), and the 2D gridded signal is shown in (c). The reconstructed image is shown in (d).

in a 1D MPI system, supported the validation of new image reconstruction strategies, described in [3]. Figure 2 shows the results of this 1D MPI simulation for different relaxation times.

A 2D MPI simulation is shown in Figure 3. A hypothetical grid (Figure 3a) was composed of *voxels* filled with 20 nm magnetite particles at a concentration of 5 mg/mL of Fe (shown in white), placed under a gradient field of 8 T/m (x direction). The time-domain raw signal (Figure 3b) is composed by the signal measured by two receive coils, aligned with the x and z axes. The gridded signal (Figure 3c) was combined with white noise, and reconstructed using the method employed in [3](Figure 3d).

IV. Conclusion

We have shown in this work the early stages of the development of a MPI simulation software which is designed to include non-ideal or experimentally determined effects of the instrument and magnetic nanoparticles. The structure adopted for the development gives flexibility for simulating a wide range of measurement configurations, including MPS, AC susceptibility and pulsed relaxometry. The assessment of the individual elements combined with the comparison against real measurements supports that the software provides reliable data. The software is ready to provide 1D and 2D, and potentially 3D temperature-dependent MPI simulation data, which will support future efforts on MNP thermometry and thermal imaging. Future improvements will focus on adding more features to the simulated systems, which includes signal filtering, noise, frequency response and non-Langevin particle magnetization.

Acknowledgments

The authors acknowledge funding from NIST's Innovations in Measurement Science grant.

Author's statement

Authors state no conflict of interest.

References

- [1] B. Gleich and J. Weizenecker. Tomographic imaging using the non-linear response of magnetic particles. *Nature*, 435(7046):1214–1217, 2005, doi:[10.1038/nature03808](https://doi.org/10.1038/nature03808).
- [2] T. Knopp, N. Gdaniec, and M. Möddel. Magnetic Particle Imaging: from Proof of Principle to Preclinical Applications. *Physics in Medicine & Biology*, 62:R124–R178, 2017, doi:<https://doi.org/10.1088/1361-6560/aa6c99>.

- [3] M.-A. Henn, K. N. Quelhas, T. Q. Bui, and S. I. Woods. Improving model-based mpi image reconstructions: Baseline recovery, receive coil sensitivity, relaxation and uncertainty estimation. *International Journal on Magnetic Particle Imaging*, submitted for publication.
- [4] N. Derby and S. Olbert. Cylindrical magnets and ideal solenoids. *American Journal of Physics*, 78,(229):229–235, 2009, doi:<https://doi.org/10.1119/1.3256157>.
- [5] J. M. Camacho and V. Sosa. Alternative method to calculate the magnetic field of permanent magnets with azimuthal symmetry. *Revista Mexicana de Física E*, 59:8–17, 2013.
- [6] T. Knopp and T. M. Buzug, *Magnetic Particle Imaging: An Introduction to Imaging Principles and Scanner Instrumentation*. Berlin/Heidelberg: Springer, 2012, doi:[10.1007/978-3-642-04199-0](https://doi.org/10.1007/978-3-642-04199-0).
- [7] T. Q. Bui, W. L. Tew, and S. I. Woods. AC Magnetometry with Active Stabilization and Harmonic Suppression for Magnetic Nanoparticle Spectroscopy and Thermometry. *Journal of Applied Physics*, 128:224901, 2020, doi:<https://doi.org/10.1063/5.0031451>.